

Simple Approach to Fabricate a Highly Sensitive H₂O₂ Biosensor by One-Step of Graphene Oxide and Horseradish Peroxidase Co-immobilized Glassy Carbon Electrode

Yue Wang^{*}, KeJuan Zhao, Zhiqiang Zhang^{*}, Hongmin Jia, Jiaqi Chen, Chen Fu

School of Chemical Engineering, University of Science and Technology Liaoning, 185 Qianshan Middle Road, High-tech zone, Anshan, Liaoning, 114501, China.

^{*}E-mail: wangyue@ustl.edu.cn, zhangzhiqiang@ustl.edu.cn

Received: 21 October 2017 / Accepted: 29 December 2017 / Published: 5 February 2018

We report a simple one-step adsorption method of horseradish peroxidase (HRP) and graphene oxide (GO) on a glassy carbon electrode (GCE) surface as a hydrogen peroxide (H₂O₂)-detecting biosensor. The surface of glassy carbon (GC) electrodes was evaluated by FT-IR spectroscopy, UV-vis spectrophotometry, atomic force microscopy (AFM), field emission scanning electron microscopy (FE-SEM) and electrochemical techniques. Under the optimum conditions, the biosensor could be successfully used for the amperometric determination of H₂O₂ in a linear concentration range of 2 μM to 500 μM with a detection limit of 1.6 μM (S/N =3), and the response time was approximately 3 s. The fabricated biosensor can avoid interference from glucose, ascorbic acid, ethanol and uric acid.

Keywords: one-step adsorption, graphene oxide, horseradish peroxidase, hydrogen peroxide.

1. INTRODUCTION

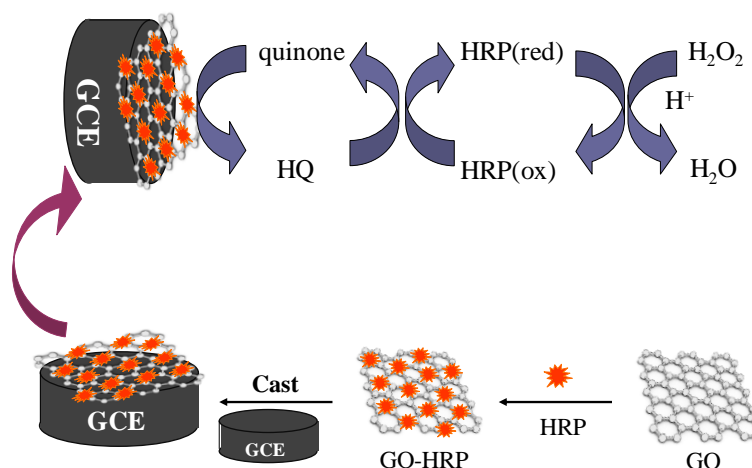
Hydrogen peroxide (H₂O₂) is widely used as an oxidizing agent in many fields, such as the clinical, pharmaceutical and food industries.[1,2] In addition, because of its redox properties, H₂O₂ is also used as a mediator in many biological and food applications.[3] However, an excessive amount of H₂O₂ has a destructive impact on the human central nervous system and can cause Parkinson's disease, Alzheimer's disease and amyotrophic lateral sclerosis.[4,5] Therefore, the accurate, sensitive, rapid, and low-cost detection of hydrogen peroxide (H₂O₂) has been particularly important and widely studied.

Various analytical techniques, including titrimetry,[6] spectrophotometry,[7] chemiluminescence,[8] chromatography and fluorescence,[9] have been carried out for the

determination of H_2O_2 . However, most of them require expensive instruments and reagents, complicated procedures and skillful techniques. Therefore, peroxidase-based biosensors are useful for the effective determination of H_2O_2 . As a member of the large class of peroxidases, horseradish peroxidase (HRP) has long been a representative enzyme. It has been used to explore the structure, dynamic and thermodynamic properties of peroxidases, particularly in understanding the biological behavior of catalyzed oxidation of substrate H_2O_2 .

The establishment of a simple, convenient and stable enzyme immobilization strategy on support matrices is an important research topic for the development of highly functional bio-devices. Among various enzyme immobilization methods, physical adsorption is one of the easiest methods and can be performed under relatively mild conditions. However, usually, physical adsorption results in a lack of operational and storage stability, which hinders its application. Furthermore, HRP is easily denatured through the direct adsorption of HRP onto a bare electrode surface and results in bioactivity loss.[10] Various functional materials, including redox mediators,[11] catalysts,[12] and proteins,[13] have been utilized to modify the surface of electrodes to construct electrochemical devices.

The use of nanomaterials for the development of biosensors has aroused considerable interest.[14] Graphene has attracted increasingly more attention since it was first reported in 2004 because of its excellent performance.[15,16] It has recently attracted tremendous interest from chemists, physicists, and materials scientists because of its extraordinary structural, thermal, mechanical, and electrical properties.[17] The amazing properties of GO are mainly derived from its unique chemical structures. It is composed of small sp^2 carbon domains surrounded by sp^3 carbon domains, and it possesses oxygen-containing hydrophilic functional groups.[18] Graphene oxide (GO) has been used as a matrix for enzyme immobilization in different biotechnological applications.[19-22]



Scheme 1. Preparation methodology and schematic representation for H_2O_2 detection of an HRP/GO/GCE biosensor

In this work, we present a simple, novel H_2O_2 biosensor by the one-step adsorption of graphene oxide (GO) and horseradish peroxidase (HRP) onto a glassy carbon surface (Scheme 1). The fabrication procedure by one-step adsorption of GO and HRP is not characterized by physical

adsorption alone. It also has the potential to form chemical covalent bonds between GO and HRP. The oxygen-containing groups on GO have can react with the amino group (-NH₂) and the carboxyl group (-COOH) of HRP. The covalent bonds may be formed between them, which enhance the stability of the GO-HRP based biosensor. Enzymatic reduction of H₂O₂ was demonstrated at the HRP-GO co-adsorbed glassy carbon electrode. The morphology of the HRP-GO-modified GCE surface was characterized by FE-SEM, AFM, UV-visible spectroscopy and electrochemical impedance spectroscopy (EIS). The electrochemical properties of HRP/GO/GCE, including electrolyte pH, applied potential, performance of the modified electrode and reproducibility of the fabrication methods have further been evaluated by electrochemical techniques.

2. EXPERIMENTAL

2.1 Reagents and chemicals

Horseshoe peroxidase (HRP, EC 1.11.1.7, >100 $\mu\text{units mg}^{-1}$) was purchased from Wako Pure Chemicals and was used as received. Graphene oxide was obtained from Suzhou TANFENG graphene Tech Co., Ltd. Hydrogen peroxide (30% (v/v)) was obtained from Sinopharm Chemical Reagent Co., Ltd. A 0.1 M phosphate buffer solution (PBS, prepared by using K₂HPO₄ and KH₂PO₄) was used to prepare the electrolyte. A standard solution of H₂O₂ was prepared immediately by the dilution of 30% H₂O₂ with buffer prior to use. All reagents were used without further purification.

2.2 Apparatus

We used field emission scanning electron microscopy (FE-SEM, ZEISS, SIGMA-HD) to image the surface of bare and modified GC electrodes. An FT-IR spectrum was recorded in the range of 500 to 4000 cm^{-1} on a Nicolet (is10) FT-IR spectrometer. UV-vis spectrophotometer (UV, Perkin Elmer, Lambda 900) was used to record the spectra of HRP, GO, and GO-HRP nanocomposites ranging from 300 to 600 nm. The AFM images were recorded with a multimode scanning probe microscope system operated in tapping mode using Being Nano-instruments CSPM-5500, Ben Yuan, Ltd. (Beijing, China). The electrochemical measurements (steady-state current and electrochemical impedance spectroscopy) were performed using an electrochemical analyzer (CHI 750D, ALS CO., Ltd) controlled by a personal computer. The steady-state current response of HRP/GO-modified GCEs was measured in a glass cell using the GC electrode as the working electrode, a platinum wire as the counter electrode, and a Ag/AgCl electrode (3 M KCl) as the reference electrode. To compare the interfacial properties of modified surfaces, EIS was performed by using deoxygenated 0.1 M phosphate buffer (pH 7.0, 15 mL) containing 1 mM Fe(CN)₆^{4-/3-}. The applied potential was set at the formal redox potential of Fe(CN)₆^{4-/3-} (i.e., 0.23 V vs. Ag/AgCl at pH 7.0). The frequency ranged from 0.01 Hz to 10 kHz. All measurements were performed in air at room temperature (~20°C). The GCE surface was polished with alumina before the fabrication of the HRP-GO nanocomposite GCE.

2.3 Preparation of modified glassy carbon electrodes

Prior to electrode modification, a glassy carbon electrode (GCE) with a diameter of 3 mm was successively polished to a mirror shine surface with 1.0 μm , 0.3 μm , and 0.05 μm alumina powder. The cleaned electrode was washed and sonicated with distilled water and ethanol to remove any adhering alumina.

Commercial graphite oxide was dispersed in PBS (5 mg/mL) and exfoliated by ultrasonication for 1 h to produce GO. The HRP-GO biocomposite was casted on the GCE surface by a one-step process. Then, 10 μL of GO dispersion (5 mg/mL) and 10 μL of HRP solution (1 mg/mL in 0.1 M PBS, pH 7) were mixed in a vial to produce the GO-HRP composite. Next, 10 μL of the GO-HRP composite was dropped onto the GCE surface, allowed to dry at room temperature and stirred/washed with distilled water to remove any loosely attached enzyme or GO particles. The HRP-GO-modified glassy carbon electrode was denoted as HRP/GO/GCE.

3. RESULTS AND DISCUSSION

3.1 Characterization of HRP-GO biocomposite

The selection and preparation of materials are extremely important in the development of electrochemical sensors. Recently, various graphene oxide composites have been analyzed to understand the performance of fabricated biosensors. The structure and functional groups of GO were examined by FT-IR spectroscopy and the results are presented in Figure. 1. The maximum peak heights at max/cm^{-1} 3210 cm^{-1} (O-H stretching), 1710 cm^{-1} (C=O stretching), 1410 cm^{-1} (O-H bending), 1100 cm^{-1} and 1030 (C-O-C stretching) are attributed to oxygen-containing functional groups on GO. The peak at 1620 cm^{-1} was ascribed to the C=C stretching, which defines the undistorted sp^2 structure of graphene oxide. These FT-IR data are consistent with the previous paper. [23] As described, GO is an excellent support for immobilized enzymes and proteins because of its solubility in water and its oxygen functionalities [24]. In addition, the large surface area of GO provides a high capacity for the immobilization of enzymes.

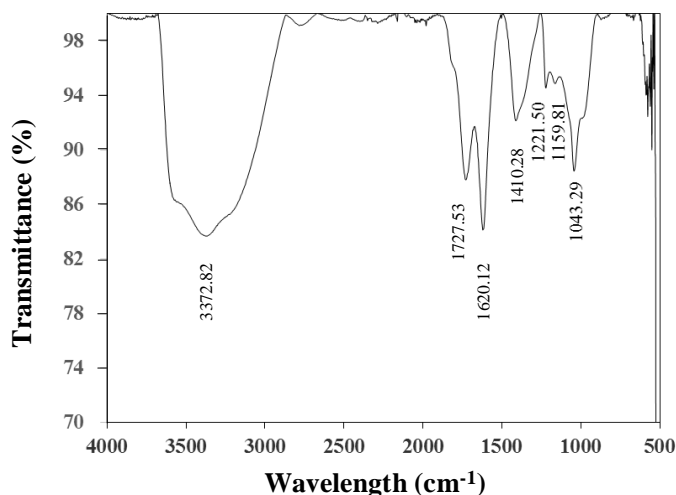


Figure 1. FT-IR spectrum of GO powder.

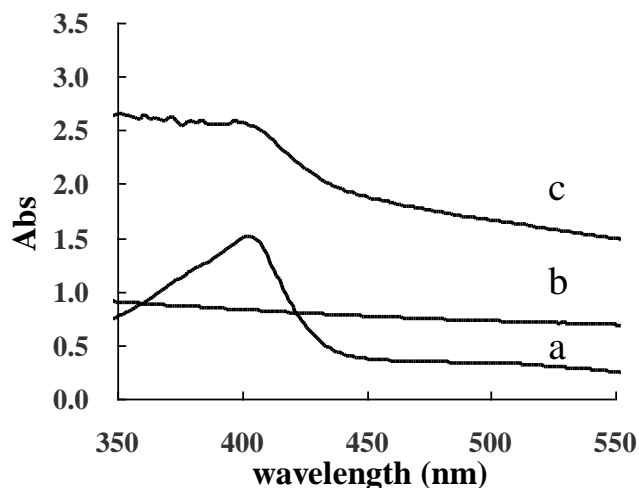


Figure 2. UV-vis absorption spectroscopy of HRP (a), GO (b) and GO-HRP mixture (c).

Heme absorption is a very useful conformational probe to study heme proteins. We can obtain information on the secondary structure of proteins by using UV-vis absorption spectroscopy. [25]

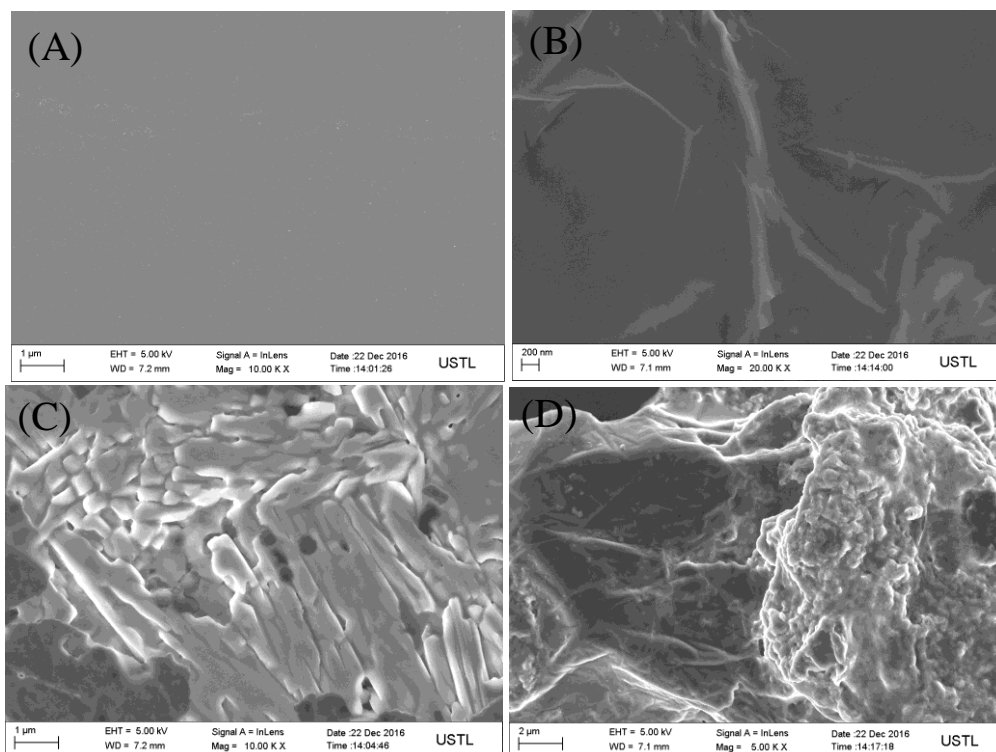


Figure 3. Field emission scanning electron microscopy (FE-SEM) images of bare GCE (A), GO-modified GCE (B), HRP-modified GCE (C) and GO-HRP-modified GCE (D).

Figure 2 shows the UV-vis absorption spectra of HRP, GO and the GO-HRP nanocomposite. The HRP solution had a Soret band centered at 403 nm (Figure 2, curve a), which is in agreement with the heme band for native HRP in phosphate buffer (pH 7.0).[26] The Soret absorption band of the GO-

HRP mixture was centered at 400 nm (Figure. 2, curve c), meaning that the absorption of the GO-HRP mixture exhibited almost no shift from the Soret absorption of the HRP film alone, and GO had no peak absorption centered at 400 nm. Figure 2 shows that the secondary structures around the heme iron of HRP adsorbed in GO composite have no significant effect when compared with HRP alone. The results indicate that HRP in the GO-HRP mixture retains its biological catalysis center of activity. The GO-HRP composite system has good biocompatibility, allowing HRP to maintain its activity. Graphene has been used in biomaterials because it can provide a biocompatible microenvironment for enzymes [27].

FE-SEM was used to evaluate the surface appearance and characteristics of the modified GCE, as shown in Figure 3. The GO-modified GCE exhibited the typical crumpled and wrinkled sheet structure of graphene oxide (figure 3B). From this result, we can find that GO has no aggregations, meaning GO dispersed uniformly in water. This kind of structure can provide a large rough surface for further enzyme immobilization. When HRP alone is used to modify the GCE surface, the plane-like surface indicates the denaturation of HRP onto the GCE surface. After GO and HRP are co-immobilized on the GCE, the GO-HRP forms a spongy film (Figure 3D), indicating the successful immobilization of HRP on the GCE surface. In addition, the morphology of HRP shown in Fig. 3D indicates that it retains its original conformation.

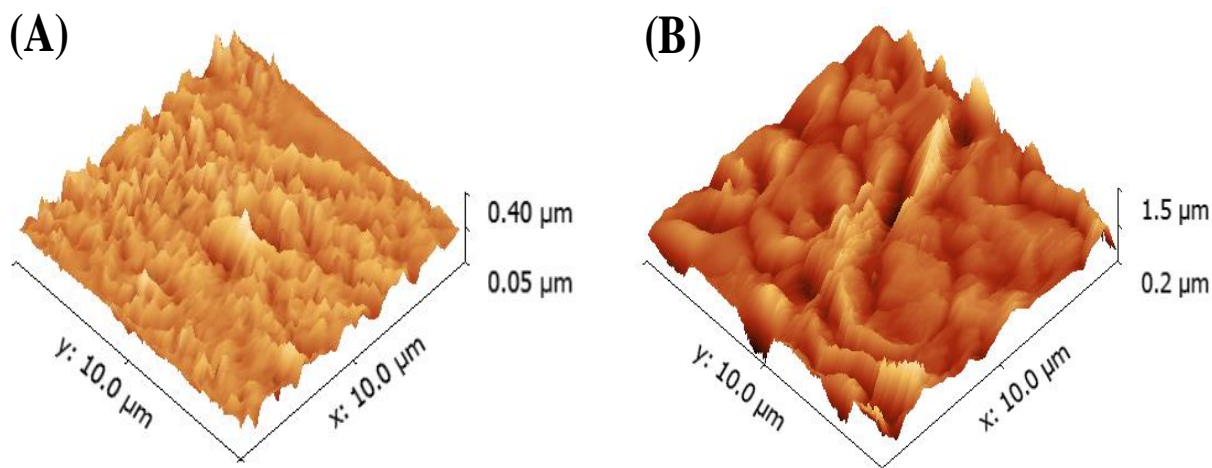


Figure 4. AFM images of the GO- and GO-HRP-modified GC electrodes and their height profile.

Figure 4 shows AFM images with the height profile of the GO- (Fig. 4A), HRP- (data not shown) and GO-HRP- (Figure 4B) modified GCEs. The heights of the GO-, HRP- and GO-HRP-modified GCEs are 400, 40.14 and 1545.3 nm, respectively. The height of the GO-HRP-modified GCE is much higher than the others. The amount of HRP was significantly increased due to the covalent bonding of GO compared with HRP immobilization only. The result is consistent with the EIS results (Figure 5). Additionally, the AFM images clearly show that the surface of a GO-modified GC electrode is rather rough than that from the GO-HRP co-immobilization procedure, which is evidence of the successful modification of HRP.

3.2 Electrochemical behavior of electrodes

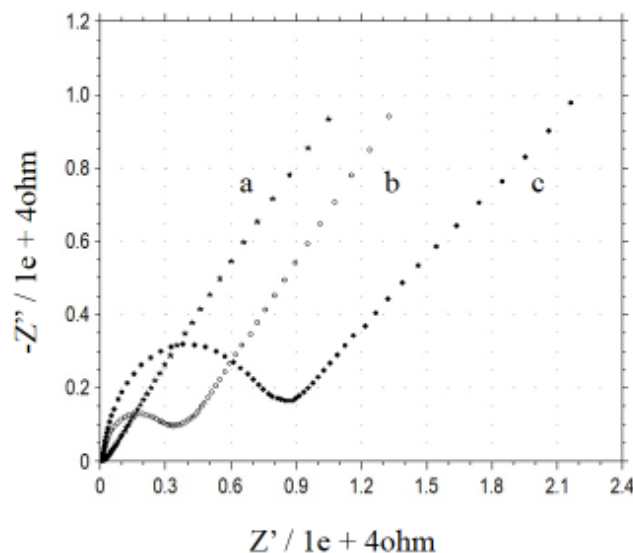


Figure 5. EIS of GCE (a), HRP/GCE (b), and HRP/GO/GCE (c) in 0.1 M PBS (pH 7.0) containing 1 mM $[\text{Fe}(\text{CN})_6]^{3-/4-}$.

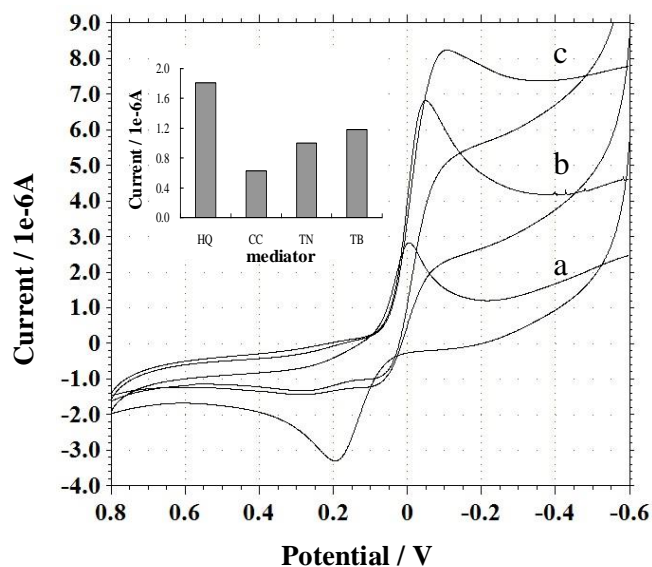


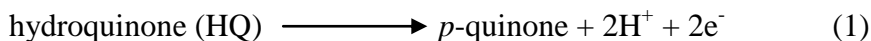
Figure 6. CVs of the HRP/GO/GCE at a scan rate of 50 mV/s in 0.1 M PBS (pH 6.5) containing 0.25 mM HQ without H_2O_2 (a) and with 0.5 and 1 mM H_2O_2 (b, c). Inset shows the current comparison of different mediators (H_2O_2 0.3 mM, mediator 0.25 mM).

EIS is a common and powerful tool for studying the interfacial properties of surface-modified electrodes. The electron transfer resistance (R_{ct}) at the electrode surface can be estimated by the Nyquist diameter. In addition, the semicircle diameter in an EIS spectrum reflects the electron transfer resistance on the electrode surface. A larger semicircle diameter means greater electron transfer resistance. Figure 5 shows the Nyquist diagrams of EIS for a bare GCE (curve a), an HRP-modified

GCE (curve b), and a GO-HRP-modified GCE (curve c). The Nyquist plot of EIS has a semicircle portion at high frequency and a linear portion at low frequency.

The EIS spectrum of the bare GCE had a very small semicircular diameter with a negligible R_{ct} value (Figure 5a), which indicates a diffusion-limited step for the $[\text{Fe}(\text{CN})_6]^{3-/4-}$ electrochemical process.[28] When the GCE was modified with HRP, the value of R_{ct} obviously increased to 4500 Ω (curve b), indicating the successful immobilization of HRP. When the GCE surface was modified with the GO and HRP mixture, the R_{ct} increased to 9000 Ω (curve c). From these data, we can speculate that GO enhances the amount of immobilized HRP, resulting in a large surface resistance.

Cyclic voltammograms (CVs) of the HRP/GO/GCE observed in the absence and presence of H_2O_2 in deoxygenated 0.1 M phosphate buffer solution (pH 6.5) containing 0.25 mM hydroquinone (HQ) are shown in Figure 6. The well-defined HQ/ p -quinone redox couple observed in the absence of H_2O_2 (curve a) was apparently changed in the presence of 0.5 and 1 mM H_2O_2 (curve b and c); the oxidation current nearly disappeared and the reduction current significantly increased (the typical catalytic current). The results clearly reveal that the HQ-mediated bio-electrocatalytic oxidation of H_2O_2 proceeds smoothly on the HRP/GO/ GCE surface. Furthermore, the mediation effects were also checked by using other mediators, which is shown in the inset of Figure 6 (*CC* catechol; *TN* thionine chloride; *TB* toluidine blue). In addition, HQ gave the best result compared with other mediators. The co-immobilization of GO and HRP on the GCE surface exhibits a sufficient bio-electrocatalytic activity with the use of HQ as an artificial electron donor according to the following scheme.[29]



3.3 Optimization of experimental conditions

The working environment is an important parameter for enzyme-based biosensors. Both strong acid and strong alkaline environments are not suitable for enzyme bioactivity. The effect of pH on the biosensor performance was studied for pH values between 5.0 and 8.5 in 0.1 M PBS. As shown in Figure 7A, the steady-state current increased from 5.0 to 6.5, and decreased from pH 6.5 to 8.5, which agrees with the behavior reported for soluble HRP.[30] Thus, the GO matrix did not change the optimum pH value for the bio-electrocatalytic reaction of immobilized HRP toward H_2O_2 . Thus, a value of 6.5 was selected as the optimized pH for the amperometric detection of H_2O_2 .

Furthermore, the applied potential was also studied, and the results are shown in Figure 7B. An overvoltage or a low voltage always results in reducing the performance of enzyme-based biosensors. The biosensor response to H_2O_2 increased with the increase in applied potential from -0.3 to -0.15 V. The highest sensitivity was obtained at -0.15 V and further increase of the anodic potential resulted in a decrease in the current response mainly due to the increased driving force for fast H_2O_2 reduction at lower potentials.[31]

3.4 Interference and selectivity

Selectivity is an important property for biosensors. It is a criterion to judge whether the biosensor is suitable for practical applications. The interferential experiment of this H_2O_2 sensor was performed to understand the selectivity of the HRP/GO/GCE biosensor. The amperometric responses with and without interferents were measured in a 0.1 M pH 6.5 phosphate buffer solution. The results showed that 10-fold amounts of glucose, uric acid, ethanol and ascorbic acid did not interfere with the determination of H_2O_2 . This result indicated good selectivity of the biosensor mainly because at the low potential used, these interfering substances cannot be electrochemically oxidized.

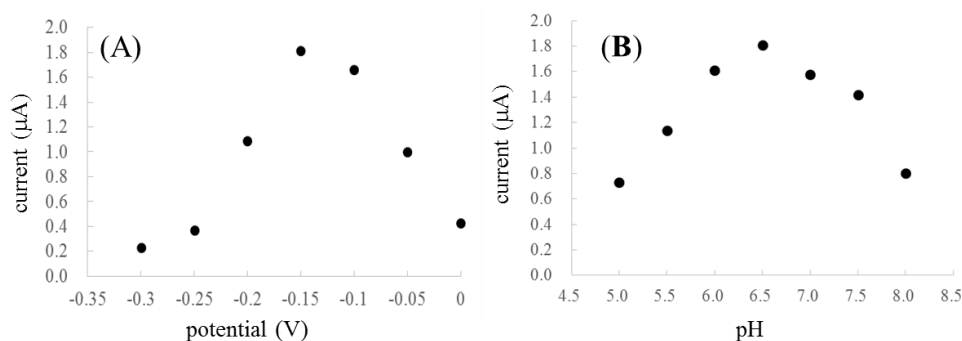


Figure 7. (A) Effect of applied potential on the amperometric response in the presence of 0.25 mM H_2O_2 in 0.1 M PBS (pH 6.5) containing 0.25 mM HQ. (B) Effect of pH on the amperometric response in the presence of 0.25 mM H_2O_2 in 0.1 M PBS (pH 6.5) containing 0.25 mM HQ, Applied potential -0.1 V.

3.5 Amperometric responses and calibration curve of the HRP/GO/GCE

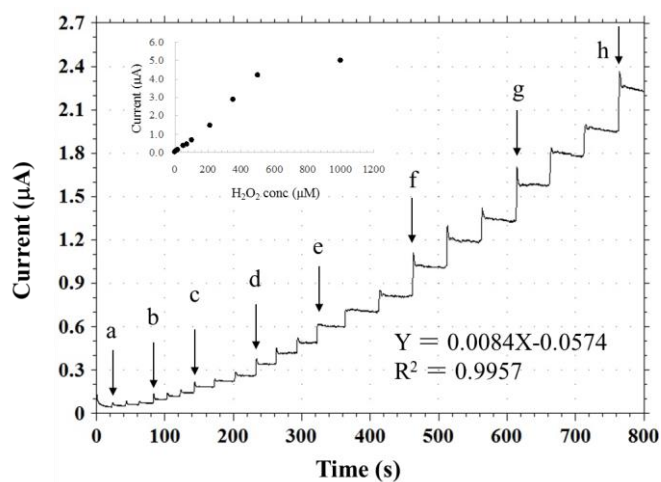


Figure 8. Steady-state response of the biosensor to the successive addition of (a) 2 μM, (b) 4.5 μM, (c) 6 μM, (d) 12 μM, (e) 18 μM, (f) 35 μM, (g) 50 μM, (h) 70 μM H_2O_2 in PBS (pH 6.5) containing 0.25 mM HQ at an applied potential of -0.15 V. Inset is the calibration plot for the current versus the concentration of H_2O_2 and the linear curve parameters.

Under the above optimal conditions, a typical amperometric response of the biosensor was measured by successively adding H_2O_2 at different concentrations, as Figure 8 shows us. The inset of Fig. 8 shows the calibration curve of the biosensor and the parameters of the linear section for the measurement of H_2O_2 . When H_2O_2 was added to the PB solution (pH 6.5), the HRP/GO/GCE biosensor responded promptly to the substrate increase and reached 95% of the steady-state current in less than 3 s.

Table 1. Response characteristics of HRP/GO/GCE biosensor to detect H_2O_2

Parameters	Sensitivity ^a ($\mu A\ mM^{-1}$)	Linear range ^a (mmol/L)	LOD ^b ($\mu mol/L$)	Correlation coefficient	Response time (s)
HRP/GO/GCE	8.4	0.002-0.5	1.6	0.9957	~ 3

^a Calculated from the slope of the calibration curve.

^b Based on a S/N ratio of 3.

Table 1 is the summary of the response characteristics of the HRP/GO/GCE-based biosensor. After calculating from the calibration curve, the sensitivity of this biosensor was determined to be 8.4 $\mu A/mM$. In addition, the response time was less than 3 s. This rapid response time is superior to carbon material-based HRP biosensors.[32-34] The linear range of the H_2O_2 detection was from 2 to 500 μM , and the detection limit was estimated to be 1.6 μM , based on the criterion of a signal-to-noise ratio of 3, which was near or better than those of the reported H_2O_2 biosensors based on the HRP biosensor (shown in Table 2). The performance was sufficient for one-step adsorption of HRP onto the GCE surface.

Table 2. Comparison between the proposed sensor and other H_2O_2 sensors based on HRP

Electrode material	Linear range (mmol/L)	LOD ($\mu mol/L$)	Reference
HRP/CNT/GA/BSA/SPE	0.005-0.1	0.85	35
HRP/SGCCN/GCE	0.495-10.6	12.89	36
HRP/sol-gel/MWCNT/GCE	0.07-3	14	37
HRP/MT-MWCNT/GCE	0.009-1	4	38
HRP/SiO ₂ /MB/gelatin/GCE	0.01-1.2	4	39
Clay/HRP/chitosan/AuNPs/GCE	0.039-3.1	9	40
HRP/chitosan/SWCNT/GCE	0.025-0.3	3	41
HRP/GO/GCE	0.002-0.5	1.6	This work

CNT: carbon nanotubes;

GA: glutaraldehyde;

BSA: bovine serum albumin;

SPE: screen printed electrode;

SGCCN: sol-gel-derived ceramic-carbon nanotube;

GCE: glass carbon electrode;

MWCNT: multi-walled carbon nanotubes;

SWCNT: single walled carbon nanotubes;
 MT: maize tassel;
 MB: methylene blue;
 AuNPs: gold nanoparticle.

As seen from Table 2, comparing several electrodes for H₂O₂ sensing, the present HRP/GO/GCE biosensor can be easily prepared by one-step physical absorption onto the GCE without any other modifying and processing procedures. The GO support provides a good biocompatible microenvironment for HRP and can retain the bioactivity of HRP. The present biosensor can detect H₂O₂ promptly, which is an advantage of biosensors for the online detection of the substrate. Furthermore, the HRP/GO/GCE biosensor has the advantages of low cost, wide linear range and low detection limit. The reproducibility of the same modified electrode was examined in 0.1 M PBS (pH 6.5) by using 40 μM H₂O₂. The relative standard deviation was 4.4% for 5 successive assays.

We measured not only the mediated current but also the direct electron transfer (DET) of HRP for the detection of H₂O₂. The GO-HRP-modified electrode showed good performance, too. The linear range of H₂O₂ detection was from 6 to 200 μM with a detection limit estimated to be 4 μM. In addition, even for the DET-base amperometric detection of H₂O₂, the present biosensor always exhibited a very fast response speed (approximately 3 s).

3.6 Analytical application

Table 3. Determination of the concentrations (mM) of H₂O₂ in disinfecting samples

Samples number	Measured by proposed H ₂ O ₂ biosensor		Measured by KMnO ₄ -titration method
	(mean ± SD) ^a	RSD%	
1	0.1025 ± 0.0045	3.0	0.1109
2	0.1978 ± 0.0335	2.6	0.2104
3	0.3163 ± 0.0455	3.4	0.3312

^a Average value from three successive measurements

To understand the practical applicability of the HRP/GO/GCE-based biosensor for real sample measurements, the biosensor was applied to determine the H₂O₂ content in a disinfecting solution. For comparison, the potassium permanganate titration method was also performed as a standard method for H₂O₂ detection. The results are shown in Table 3. Under the optimized conditions, the present biosensor is still effective and accurate for the detection of H₂O₂ in disinfecting samples within the linear range. The results mean that the present biosensor has potential for further applications.

4. CONCLUSIONS

A simple electrochemical H₂O₂ biosensor was designed by the co-immobilization of HRP and GO on a glassy carbon electrode. The fabrication procedure includes a chemical adsorption process. The HRP molecules retained their native secondary structures around the heme iron of the HRP-GO mixture. The GO matrix has the following advantages: 1) provides a good biocompatible

microenvironment, 2) retains the conformation and biological activity of HRP molecules, 3) enhances the amount of HRP on the electrode surface. The GO/HRP/GCE biosensor can catalyze both direct electron transfer and mediated-electron transfer of H₂O₂. The biosensor showed a high sensitivity, short response time (3 s), and good linear relationship for H₂O₂ detection. The linear range is from 2 to 500 μM with a limit of detection of 1.6 μM (S/N =3) for the mediated-current response. Additionally, the GO/HRP/GCE biosensor can detect H₂O₂ through the direct electron transfer route. The fabrication method of the HRP biosensor is simple and can be applied to other enzyme-based biosensors, but more work is needed to obtain a wider linear range and excellent stability.

ACKNOWLEDGMENTS

The authors gratefully acknowledge the financial support from the Natural Science Foundation of Liaoning Province (No. 20170540464), the department of education of Liaoning (No. 2017LNQN05) and the Foundation of University of Science and Technology, Liaoning (No. 2015QN08 and No. 2016RC12).

References

1. S.H. Chen, R. Yuan, Y. Chai and F. Hu, *Microchim Acta*, 180 (2013) 15.
2. Y. Li, J.J. Zhang, J. Xuan, L.P. Jiang and J.J. Zhu, *Electrochem. Commun.*, 12 (2010) 777.
3. X. Shi, W. Gu, B. Li, N. Chen, K. Zhao and Y. Xian, *Microchim Acta*, 181 (2014) 1.
4. S.J. Li, J.M. Du, J.P. Zhang, M.J. Zhang and J. Chen, *Microchim Acta*, 181 (2014b) 631.
5. Y. Luo, H. Liu, Q. Rui and Y. Tian, *Anal. chem.*, 81 (2009) 3035.
6. N.V. Klassen, D. Marchington and H.C.E. McGowan, *Anal. Chem.*, 66 (1994) 2921.
7. C. Matsubara, N. Kawamoto and K. Takamura, *Analyst*, 117 (1992) 1781.
8. M.P. Wymann, V. Tschärner, D.A. Deranleau and M. Baggiolini, *Anal. Biochem.*, 165 (1987) 371.
9. T.R. Holm, G.K. George and M.J. Barcelona, *Anal. Chem.*, 59 (1987) 582.
10. Z.J. Wang, M.Y. Li, P.P. Su, Y.J. Zhang, Y.F. Shen, D.X. Han, A. Ivaska and L. Niu, *Electrochem. Commun.*, 10 (2008) 306.
11. B. Wang and J. Anzai, *Langmuir*, 23 (2007) 7378.
12. H. Shi, Y. Yang, J. Huang, Z. Zhao, X. Xu, J. Anzai, T. Osa and Q. Chen, *Talanta*, 70 (2006) 852.
13. Y. Wang, Y. Hasebe, *Sens Actuators B*, 155 (2011) 722.
14. W. Yang, K. R. Ratinac, S. P. Ringer, P. Thordarson, J. J. Gooding and F. Braet, *Angew Chem.*, 49 (12) (2010) 2114.
15. K.S. Novoselov, A.K. Geim, S.V. Morozov, D. Jiang, Y. Zhang, S.V. Dubonos, I.V. Grigorieva and A.A. Firsov, *Science*, 306 (5969) (2007) 666.
16. W. Lei, W. Si, Y. Xu, Z. Gu and Q. Hao, *Microchim Acta*, 181 (2014) 707.
17. S.P. Lonkar, Y.S. Deshmukh and A.A. Abdala, *Nano research*, 8 (2015) 1039.
18. K.P. Loh, Q. Bao, G. Eda and M. Chhowalla, *Nat. Chem.*, 2 (2010) 1015.
19. B. Unnikrishnan, S. Palanisamy and S.M. Chen, *Biosens. Bioelectron.*, 39 (2013) 70.
20. B. Liang, L. Fang, G. Yang, Y.C. Hu, X.S. Guo, X.S. Ye, *Biosens. Bioelectron.*, 43 (2013) 131.
21. A.S. Campbell, Y.J. Jeong, S.M. Geier, R.R. Koepsel, A.J. Russell and M.F. Islam, *ACS Appl Mater Interfaces*, 7 (2015) 4056.
22. X. Sun, Z. Liu, K. Welsher, J.T. Robinson, A. Goodwin, S. Zaric and H.J. Dai, *Nano Res.*, 1 (2008) 203.
23. J. Chen and Y.L. Jin, *Microchim Acta*, 169 (2010) 249.
24. P. Bolibok, M. Wiśniewski, K. Roszek, A.P. Terzyk, *Sci. Nat.*, 104 (2017) 36.

25. C.L. Guo, Y.H. Song, H. Wei, P.C. Li, L. Wang, L.L. Sun, Y.J. Sun and Z. Li, *Anal. Bioanal. Chem.*, 389 (2007) 527.
26. N.Q. Jia, Q. Zhou, L. Liu, M.M. Yan and Z.Y. Jiang, *J Electroanal. Chem.*, 580 (2005) 213.
27. B. Liang, L. Fang, G. Yang, Y. Hu, X. Guo, X. Ye, *Biosens. Bioelectron.* 43 (2013) 131.
28. Z.F. Yao, X. Yang, F. Wu, W.L. Wu and F.P. Wu, *Microchim Acta*, 183 (2016) 2799.
29. B.X. Gu, X.C. Xu, G.P. Zhu, S.Q. Liu, L.Y. Chen, M.L. Wang and J.J. Zhu, *J Phys Chem B*, 113 (2009) 6553.
30. H. Harbury, *J Biol. Chem.*, 225 (1957) 1009.
31. J.B. Jia, B.W. Wang, A.G. Wu, G.J. Cheng, Z. Li and S.J. Dong, *Anal. Chem.*, 74 (2002) 2217.
32. L.Q. Luo, L.M. Zhu, Y.H. Xu, L.Y. Shen, X. Wang, Y.P. Ding, Q.X. Li, D.M. Deng, *Microchim Acta*, 174 (2011) 55.
33. H.J. Jiang, C. Du, Z.Q. Zou, X.W. Li, D.L. Akins, H. Yang, *J Solid State Electrochem.* 13 (2009) 791.
34. G.S. Lai, H.L. Zhang, D.Y. Han, *Microchim Acta*, 165 (2009) 159.
35. S.X. Xu, X.J. Qin, X.F. Zhang and C.X. Zhang, *Microchim Acta*, 182 (2015) 1241.
36. X.H. Kang, J. Wang, Z.W. Tang, H. Wu and Y.H. Lin, *Talanta*, 78 (2009) 120.
37. S. X. Xu, J. L. Li, Z. L. Zhou, C. X. Zhang, *Anal Methods*, 6 (2014) 6310.
38. M. Moyo, J.O. Okonkwo and N.M. Agyei, *Electroanal.*, 25 (2013) 1946.
39. H. Yao, N. Li, S. Xu, J.Z. Xu, J.J. Zhu and H.Y. Chen, *Biosens. Bioelectron.*, 21 (2005) 372.
40. X.J. Zhao, Z.B. Mai, X.H. Kang and X.Y. Zou, *Biosens. Bioelectron.*, 23 (2008) 1032.
41. H.J. Jiang, C. Du, Z.Q. Zou, X.W. Li, D.L. Akins, H. Yang, *J. Solid State Electrochem*, 13 (2009) 791.

© 2018 The Authors. Published by ESG (www.electrochemsci.org). This article is an open access article distributed under the terms and conditions of the Creative Commons Attribution license (<http://creativecommons.org/licenses/by/4.0/>).